Journal of Applied & Environmental Microbiology, 2014, Vol. 2, No. 5, 220-230
Available online at http://pubs.sciepub.com/jaem/2/5/4

DOI:10.12691/jaem-2-5-4

Effect of 3-Chloroaniline in Microbial Community Structure of Activated Sludge

M. Shah*

Industrial Waste Water Research Laboratory Division of Applied & Environmental Microbiology Enviro Technology Limited Gujarat, India
*Corresponding author: shahmp@uniphos.com

Received June 16, 2014; Revised July 06, 2014; Accepted July 16, 2014

Abstract Present work evaluated the effects on activated-sludge reactor functions of a 3-chloroaniline (3-CA) pulse and bioaugmentation by inoculation with the 3-CA-degrading strain Pseudomonas stuzeri. Changes in functions such as nitrification, carbon removal, and sludge compaction were studied in relation to the sludge community structure, in particular the nitrifying populations. Denaturing gradient gel electrophoresis (DGGE), real-time PCR, and fluorescent in situ hybridization (FISH) were used to characterize and enumerate the ammonia-oxidizing microbial community immediately after a 3-CA shock load. Two days after the 3-CA shock, ammonium accumulated, and the nitrification activity did not recover over a 12-day period in the non bioaugmented reactors. In contrast, nitrification in the bioaugmented reactor started to recover on day 4. The DGGE patterns and the FISH and real-time PCR data showed that the ammonia-oxidizing microbial community of the bioaugmented reactor recovered in structure, activity, and abundance, while the number of ribosomes of the ammonia oxidizers in the nonbioaugmented reactor decreased drastically and the community composition changed and did not recover. The settle ability of the activated sludge was negatively influenced by the 3-CA addition, with the sludge volume index increasing by a factor of 2.3. Two days after the 3-CA shock in the non bioaugmented reactor, chemical oxygen demand (COD) removal efficiency decreased by 36% but recovered fully by day 4. In contrast, in the bioaugmented reactor, no decrease of the COD removal efficiency was observed. This study demonstrates that bioaugmentation of wastewater reactors to accelerate the degradation of toxic chlorinated organic such as 3-CA protected the nitrifying bacterial community, thereby allowing faster recovery from toxic shocks.

Keywords: *chloroaniline, Pseudomonas stutzeri, COD, ribosome*

Cite This Article: M. Shah, "Effect of 3-Chloroaniline in Microbial Community Structure of Activated Sludge." *Journal of Applied & Environmental Microbiology*, vol. 2, no. 5 (2014): 220-230. doi: 10.12691/jaem-2-5-4.

1. Introduction

Nowadays, biological wastewater treatment plants (WWTPs) are the most common biotechnological application in the world [1]. From the various alternatives of biological treatment systems that exist, conventional activated sludge (CAS) bioreactors are by far the most commonly used secondary treatment technology [2]. Despite of periodic improvements to the technology since its invention almost a century ago [2] and its ubiquitous global application, little is known about the underlying factors controlling the complex dynamics of the microbial populations interacting in the bioreactors and how those dynamic interactions affect the system's functional stability [3]. Until recently, a major obstacle was that the science behind most of those technology improvements was almost entirely empirical rather than theoretical [2,4]. Major changes to the design of CAS systems were done predominantly from an engineering perspective, greatly underestimating the importance of microbial communities as an integral component of these biological treatment systems [2,5]. Thus, many essential aspects regarding the ecology and dynamics of microbial communities within these systems, necessary for a rational improvement of their design and operation, remain unresolved [5]. Recent efforts have focused on improving the treatment process from a bio-ecological perspective, but so far few studies have been able to establish a clear link between the structure and function of microbial communities and the design and operation of the bioreactors [6]. Most of these efforts have failed due to limiting methodology issues. One of these issues is the modeling of full scale WWTP bioreactors based on studies of lab-scale and pilot scale bioreactors [6,8]. These studies have often been misleading and far from mimicking the real conditions observed in full-scale bioreactors, creating a big gap between their theoretical and their practical contributions [9,10]. Another issue is that many studies had focused on analyzing single bioreactors [11,12], neglecting from their analysis the effect that niche-specific factors may play in the structure and function of microbial communities [4,13,14]. The most notorious, and therefore highly scrutinized, of these issues is culture- and traditional-microscopy-based studies. These studies, aimed to

elucidate the diversity of microbes in WWTPs [15,16,17,18], proved to be unreliable, irreproducible and created erroneous perceptions of the dominant populations in the bioreactors [19,20,21,22]. They also failed to consider operational and geographical factors on the composition of the communities [23,24,25,26]. With the development and application of modern culture independent molecular techniques in ecological studies of wastewater treatment systems [20,27,28,29], the capacity of researchers to understand the true dynamics of microbial communities in these ecosystems has greatly been improved [10]. However, de los Reyes [30] explains that advanced molecular studies of microbial communities in WWTPs have led to the emergence of a microbial community ''structure-function'' paradigm that has not yet been fully clarified. Linking changes in system design and operation with the ecological factors controlling community assembly in the bioreactors will be critical in fully clarifying this ''structure function'' paradigm and resolving important operational issues, such as: sludge bulking (e.g. [31]), poor biochemical removal (e.g. [32]), and system instability (e.g. [33,34]); ultimately resulting in more stable and predictable systems [4]. Moreover, the study of CAS systems could provide, in turn, a research platform for developing and validating ecological principles that could be used to predict the behavior of microbial communities in other engineered and natural ecosystems [35,36,37]. In this study, another molecular biology technique, the amplified ribosomal DNA restriction analysis (ARDRA), is applied to activated sludge samples. Even faster than hybridization and probing, ARDRA has been used in the analysis of mixed bacterial populations from different environments [38,39,40]. The aim of this work was to evaluate the short-term effects of a 3-CA shock load and bioaugmentation with 3-CA-degrading inoculants on reactor functions such as nitrification, carbon removal, and sludge compaction. Denaturing gradient gel electrophoresis (DGGE), FISH, and real-time PCR were used to examine the changes in the structure, abundance, and activity of the nitrifying community.

2. Materials and methods

2.1. Semi Continuous Activated Sludge reactors.

The experiments were conducted with sludge freshly collected from industrial effluent wastewater treatment plant by using a modified Semi Continuous Activated Sludge procedure [41]. In brief, every 2 days, 200 ml of the mixed liquor was removed from the reactors (in 2-liter plastic Erlenmeyer flasks with an active volume of 1.0 liters) and 1.0 liter was allowed to settle for 30 min in an Imhoff cone, of which the upper 400 ml of the effluent was removed for analysis. The remaining settled sludge was poured back into the respective reactor, together with 600 ml of synthetic influent volumetric loading rate of 1 g of chemical oxygen demand [COD] liter^{-1} day^{-1}; COD/N/P ratio of 100:6:1) to bring the active reactor volume back to 1.2 liters. The SCAS reactors operated with a hydraulic retention time of 4 days and a sludge retention time of 12 days and contained 4 g of suspended solids liter^{-1}. To analyze sludge volume (SV), 1 liter of the mixed liquor was allowed to settle for 30 min in an Imhoff cone [42]. The sludge volume index (SVI) was calculated by dividing the SV by the suspended solids (SS) [42]. All reactors were operated for 6 days before the experiment in order to allow the reactors to stabilize. On day 0, reactors 1 (n = 2) continued to receive only milk powder and were control reactors. In addition to the milk powder, reactors 2 (n = 2) and 3 (n = 2) both received on day 0 a shock load of 300 mg of 3-CA resulting in a final concentration of 250 mg liter^{-1} in the reactor mixed liquor. The bioaugmentation experiment was performed in reactors 3, in which *Pseudomonas stutzeri* was inoculated. This strain, which has been chromosomally marked with *amp* (the gene encoding green fluorescent protein), mineralizes 3-CA, fluoresces green under UV light and is rifampin (100 µg/ml) as well as kanamycin (50 µg/ml) resistant [41,42]. Luria broth (LB) agar supplemented with rifampin (100 mg liter^{-1}) and kanamycin (50 mg liter^{-1}) was used to count *Pseudomonas stuzeri amp [41]*. The *Pseudomonas stuzeri amp* inoculum was grown overnight at 28°C in 5 ml of LB medium (1 liter contains 5 g of NaCl, 10 g of tryptone, and 5 g of yeast extract) containing 100 mg of 3-CA liter^{-1}. Subsequently, 5-ml cultures were used to inoculate 200 ml of LB medium plus 3-CA (100 mg liter^{-1}). After overnight incubation at 28°C in a shaker (140 rpm; New Brunswick Scientific), the cultures were centrifuged (1 min at 5,000 x g), washed twice with saline (0.85% NaCl), and finally resuspended in saline. Reactors 3 were inoculated with *Pseudomonas stuzeri amp* to a final concentration of (5.4 ± 0.37) x 10^8 cells/ml.

2.2. Sampling

Every 2 days, a sample was taken for high-performance liquid chromatography (HPLC) analysis, for DNA and RNA extraction, for FISH analysis, for plate counts of s *Pseudomonas stuzeri amp*, and for determination of the SS and SVI [42]. For DNA and RNA isolation, aliquots of the samples were immediately frozen at ⁻20 and ⁻80°C, respectively. For FISH, a subsample of activated sludge was fixed overnight with 4% paraformaldehyde [43].

2.3. Analytical methods

The effluent was analyzed for 3-CA content by reversed phase HPLC after centrifugation at 5,000 x g for 10 min. The Summit HPLC system (Dionex, Wommelgem, Belgium) consisted of a Dionex pump series P580, a Dionex autosampler model ASI-100 (injection volume, 20 µl), an STH585 column oven (at 28°C), a Dionex UV/VIS UVD 340S detector, and Chromeleon software system version 6.10. A Hypersil Green Env column (150 by 8 mm [inner diameter]; 5-µm particle size] was used. The mobile phase consisted of CH3OH–0.1% H3PO4 (ratio, 70:30), with a flow rate of 0.8 ml/min. The UV detector was used at 210 nm. The effluent was analyzed for nitrite, nitrate, and ammonium content by ion chromatography after centrifugation at 5,000 x g for 10 min and filtration through a 0.45-µm-pore-size filter. The DX-600 system (Dionex) consisted of a Dionex pump series GP50, a Dionex autosampler model AS50 (injection volume, 100 µl), a Dionex ED50 electrochemical detector, and PeakNet 6 software system version 6.10. Ionpac AS9-HC (250 by 4 mm [inner diameter]; 9-µm particle size [Dionex]) column

and Ionpac CS12-HC (250 by 4 mm [inner diameter]; 8-µm particle size [Dionex]) were used for anion and cation separation, respectively. The mobile phase consisted of Na_2CO_3 (9 mM) and methane sulfonic acid (20 mM) for anion and cation analysis respectively, with a flow rate of 1 ml/min. The residual COD and SVI of the effluent were determined by standard methods (24).

2.4. DNA and RNA Extraction from Activated Sludge

Total DNA extraction from the sludge samples and PCR conditions were based on the protocols described previously [41]. The total RNA extraction protocol was adapted from those of Griffiths et al. [44] and Kowalchuk et al. [45]. Briefly, in a 2-ml Eppendorf tube, 0.5 g of RNase-free 0.1-mm-diameter zirconia/silica beads, 0.5 ml of activated sludge, 0.5 ml of CTAB buffer (5% [wt/vol] hexadecyl trimethylammonium bromide, 0.35 M NaCl, 120 mM potassium phosphate buffer [pH 8.0]), and 0.5 ml of phenol-chloroformisoamyl alcohol mixture (25:24:1) were homogenized three times for 30 s each at 5,000 rpm in a Bead beater with 10 s between shakings. Eppendorf tubes were spun centrifuged (5 min at 3,000 x *g*), and 300 µl of the supernatant was transferred to an RNase-free Eppendorf tube. Another 500 µl of CTAB buffer was added to the sludge suspension and homogenized again three times for 30 s each at 5,000 rpm in the Bead beater with 10 s between shakings. Then 300 µl of the supernatant was added to the 300 µl taken from the first extraction, for a total of 600 µl. The phenol was removed by mixing with an equal volume of chloroform-isoamyl alcohol (24:1), inverting the tube, and centrifuging for 10 s. The upper, aqueous phase was transferred to a new Eppendorf tube, and nucleic acids were precipitated with 2 volumes of 30% (wt/vol) polyethylene glycol 6000–1.6 M NaCl for 2 h at room temperature. The Eppendorf tube was then centrifuged at 18,000 x *g* in a refrigerated centrifuge at 4 °C for 10 min. The nucleic acid pellet was subsequently washed in ice-cold 70% (vol/vol) ethanol and dried under vacuum for 10 min before being resuspended in 100 µL of RNase-free water. To obtain pure RNA a RQ1 RNase-Free DNase treatment was performed as specified by the manufacturer (Promega, Madison, Wis.). The average RNA yield was 3.4 ng ml of activated sludge^{-1}.

2.5. RT-PCR and PCR

The RNA was reverse transcribed to cDNA by using the Moloney murine leukemia virus (M-MLV) reverse transcriptase kit (Promega). Briefly, for each sample, 1 µl of each 10 mM deoxy nucleoside triphosphate solution, 1 µl of random hexamer primers (Sigma), 1 µl of extracted RNA, and 7 µl of DNase- and RNase-free filter-sterile water (Sigma) were mixed, incubated at 70°C for 10 min, and placed on ice. To each sample, a mixture was added containing 4 µl of 5x first-strand buffer (Promega), 2 µl of 0.1 Mdithiothreitol (Promega), 1 µl of M-MLV reverse transcriptase (Promega), 0.5 µl of RNase inhibitor (Sigma), and 2.5 µl of DNase and RNase-free filter-sterile water (Sigma). The sample, containing a final vol-ume of 20 µl, was incubated subsequently at 25°C for 10 min, 37°C for 3 h, and 94°C for 10 min. The cDNA was stored at 4°C (short-term storage) or ⁻20°C (long-term storage). A 1-µl volume of the DNA or cDNA was amplified as previously described [46]. A list of the primers used in this study is given in Table 1. In brief, the 16S rRNA or rDNA for all members of the *Bacteria* were amplified by PCR using the forward primer P338F and the reverse primer P518r, and a GC-clamp of 40 bp was added to the forward primer. To amplify the 16S rDNA of the AOB, which belong to the β-*Proteobacteria*, a nested PCR approach was used. In the first PCR round, the forward primers were CTO189fAB and CTO189fC and the reverse primer was CTO653r, and in the second PCR round, primers P338F and P518r were used. After the first PCR round, a clearly visible band was present (the first PCR product was at least 0.3% of the total extracted DNA or cDNA), which suggested that no nonspecific amplification was expected in the second round [46]. For more information about the specificity of the probes and primers listed in Table 1, see references 40 and 50.

Table 1. Sequences of the primers and probes used in this study

Primer or probe	Target	Sequence (5'→ 3')	Reference
Primers			
P338F	*Bacteria*	ACTCCTACGGGAGGCAGCAG	81
P518r	Universal	ATTACCGCGGCTGCTGG	81
CTO189AB	*β-Proteobacteria* ammonia oxidizers	GGAGRAAAGCAGGGGATCG	45
CTO189C	*β-Proteobacteria* ammonia oxidizers	GGAGGAAAGTAGGGGATCG	
CTO653r	*β>-Proteobacteria* ammonia oxidizers	CTAGCYTTGTAGTTTCAAACG	45
GC-clamp		CGCCGGGGGCGCGCCCCGGGCGGGGCGGGGGCACGGGGGG	47
Probes			
NSO 190	*β-Proteobacteria* ammonia oxidizers	CGATCCCCTGCTTTTCrCC	32
EUB338	Most bacteria	GCTGCCTCCCGTAGGAGT	83
EUB338 II	*Planctoniycetales*	GCAGCCACCCGTAGGTGT	84
EUB338 III	*Vemicomicrobiales*	GCTGCCACCCGTAGGTGT	34

2.6 DGGE Analysis

DGGE based on the protocol of Muyzer et al. [47] was performed using the Bio-Rad D gene system. PCR fragments were loaded onto 8% (wt/vol) polyacrylamide gels in 1xTAE (20 mM Tris, 10 mM acetate, 0.5 mM EDTA [pH 7.4]). On each gel, a home-made marker of different PCR fragments was loaded, which was required for processing and comparing the different gels [46]. The polyacrylamide gels were made with denaturing gradients ranging from 50 to 65% [41]. The electrophoresis was run for 17 h at 60°C and 38 V. Staining and analysis of the gels were performed as described previously [41]. Normalization and analysis of DGGE gel patterns were done with BioNumerics software version 2.0 (Applied Maths, Kortrijk, Belgium). During this processing, the different lanes are defined, background is subtracted, differences in the intensity of the lanes are compensated

during normalization, and bands and band classes are detected. The band classes of the DGGE patterns were exported to EstimateS [48], a program which allows statistical analysis of species richness from samples by calculating the Chao2 index [49] using the equation Chao2 = S_{obs} + ($L^2/2M$), where S_{obs} is the observed number of species in a sample, L is the number of species that occur in only one sample ("unique species"), and M is the number of species that occur in exactly two samples. This is an incidence-based nonparametric estimator that uses presence absence data and can be used with 16S rRNA-DGGE patterns to obtain a first estimate of the community richness, making it a suitable index for PCR based analysis [50,51]. The calculation of the matrix of similarities is based on the Pearson product moment correlation coefficient. The clustering algorithm of unpaired pair group method using arithmetic averages (UPGMA) was used to calculate dendrograms. Relevant and nonrelevant clusters were separated by the statistical cluster cutoff method (BioNumerics Manual 2.5).

2.7. Real-Time PCR

The real-time PCR was based on the principle of Heid et al. [52]. For quantification of AOB by real-time PCR, amplification was performed in 25-µl reaction mixtures by using buffers supplied with the qPCRT core kit for SybrT Green I in Micro Amp Optical 96-well reaction plates with optical caps. Primers CTO189fAB, CTO189fC, and CTO653r and primers P338F and P518r (Table 1) were used for the quantification of AOB and the *Bacteria*, respectively, at a concentration of 300 nM. The PCR temperature program was as follows: 50°C for 2 min and 95°C for 5 min, followed by 40 cycles of 95°C for 15 s, 53°C (all *Bacteria*) or 57°C (AOB) for 30 s, and 60°C for 1 min. The template cDNA in the reaction mixtures was amplified (n = 3) and monitored with an ABI Prism SDS 7000 instrument. Standard curves constructed after real-time PCR amplification of five different DNA concentrations (n = 4) ranging from 5.0 x 10^5 to 5.0 x 10^3 copies of DNA/well were used. A 667-bp M13 PCR fragment of a *Nitrosomonas* sp. sequence was generated as a template for the standard curve. The $r2$ values were greater than 0.99 for both standard curves, and slopes of $^{-}$3.87 and $^{-}$3.68 were generated for AOB and all *Bacteria*, respectively. The relative number of rRNA molecules of the AOB was determined by dividing the number of AOB rRNA copies by the total number of bacterial rRNA molecules.

2.8. Fish

Sludge samples were fixed with fresh 4% paraformaldehyde solution, washed with phosphate-buffered saline, and stored in phosphate-buffered saline–ethanol (1:1) at -20°C until further processing [43]. FISH assays were performed with fluorescently labeled, rRNA-targeted oligonucleotide probes by the method of Biesterfeld et al. [53]. The following oligonucleotide probes were used (Table 1): (i) NSO190, specific for the AOB (labeled with sulfoindocyanine dye Cy3) and (ii) a mix of EUB338, EUB338-II, and EUB338-III, specific for the domain *Bacteria* (labeled with fluoresceine). Samples were analyzed by standard epifluorescence microscopy on an Axioskop II microscope (Carl Zeiss, Jena, Germany). Quantification of cells was based on the procedure described by Daims et al. [54]. In brief, TIFF files were exported by the image acquisition software and analyzed with MicroImage 4.0. For each reactor from each day, five random pictures were recorded. The area fraction of stained AOB cells was calculated as a percentage of the total area of bacteria, stained with the EUB338 probe mix.

2.9. DNA Sequencing

16S rDNA gene fragments were cut out of the DGGE gel with a clean scalpel and added to 50 µl of PCR water. After 12 h of incubation at 4°C, 1 µl of the PCR water was reamplified with primer set P338F and P518r. Then 5 µl of the PCR product was loaded onto a DGGE gel (see above), and if the DGGE pattern showed only one band, it was sent out for sequencing. DNA sequencing of the ca. Analysis of DNA sequences and homology searches were completed with standard DNA sequencing programs and the BLAST server of the National Center for Biotechnology Information (NCBI) using the BLAST algorithm.

3. Results

3.1. Semi Continuous Activated Sludge Reactor Performance

Three different pairs of reactors were examined. The first pair of reactors was used as a control, with no inoculation or shock load applied (reactors 1). The second pair consisted of the 3-CA-treated reactors (disturbed reactors); they received a shock load treatment of 3-CA on day 0 (reactors 2). The third pair of reactors was the bioaugmented reactors, which received the same 3-CA pulse on day 0 but were also inoculated with *Pseudomonas stutzeri amp* cells (reactors 3). The number of *Pseudomonas stutzeri amp* cells decreased ca. 3 log units after inoculation and stabilized after 6 days at 105 CFU ml^{-1} (Figure 1A). As a result of the inoculation in reactors 3, the *Pseudomonas stutzeri amp* cells had removed all detectable 3-CA 48 h after inoculation (Figure 1B). In reactors 2 without *Pseudomonas stutzeri amp*, 3-CA persisted until day 6, and its removal was due solely to washout (the hydraulic retention time of the system was 4 days) and not to (bio) degradation. The 3-CA shock inhibited nitrification for an extended period despite its disappearance by day 2 in the protected reactors and day 6 in the non bioaugmented reactors (Figure 1C and D). In non bioaugmented reactors 2, nitrite and nitrate concentration remained very low and ammonium accumulated for the duration of the experiment. From day 4, nitrification in the bioaugmented reactors 3 recovered, resulting in the accumulation of nitrate (Figure 1C) and nitrite (Figure 1D). The nitrite was present in reactors 3 until day 6, but by day 8, all the nitrite was removed. The restored nitrification activity resulted in the complete removal of ammonium from day 6 (Figure 1D). In both reactors that received the 3-CA pulse, the SVI increased, indicating that the settlement of the activated sludge was poor (Figure 1E). In contrast to nitrification, the SVI did not recover in the bioaugmented reactors during the first 10 days; however, the sludge compactability improved on day 12. Only the non bioaugmented shock-loaded reactors

2 accumulated large amounts of COD (Figure 1F). However, from day 4, COD removal increased again. The bioprotection of reactors 3 was very effective, and no differences in COD removal compared to control reactors 1 were observed.

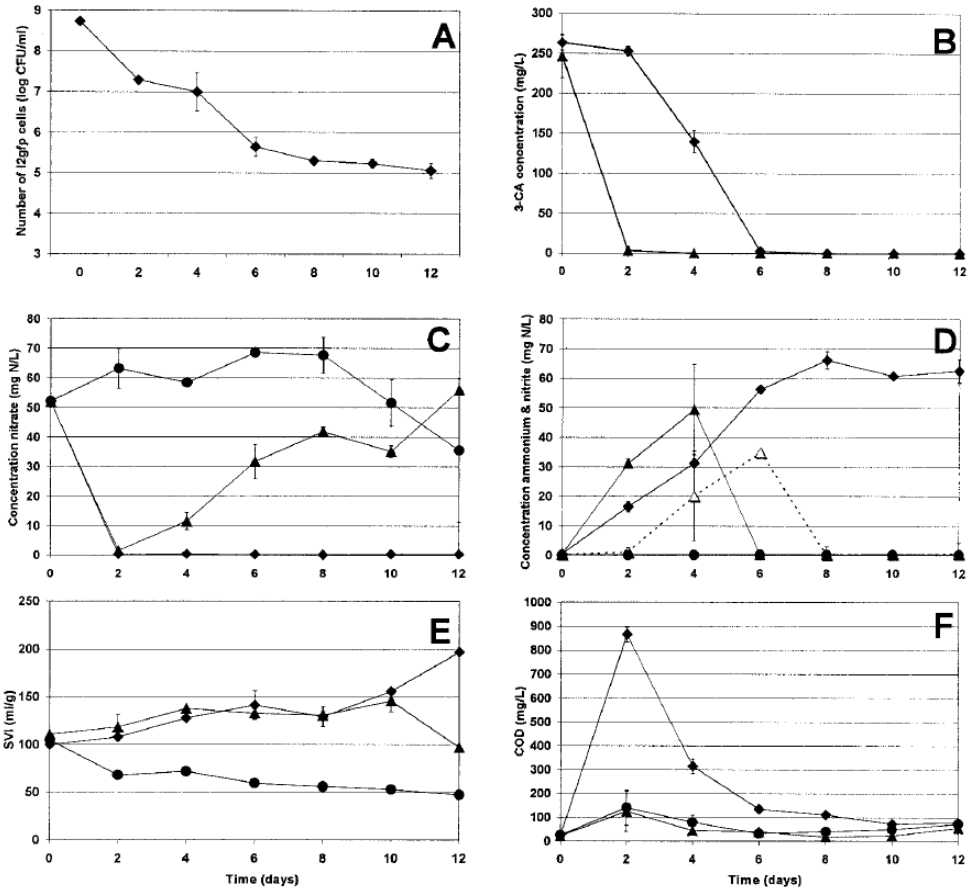

Figure 1. Data obtained from the different types of reactors. Reactors 1 were not bioaugmented, and no 3-CA shock was applied (•); reactors 2 were not bioaugmented but were exposed to a 3-CA shock load (♦); reactors 3 were bioaugmented and exposed to a 3-CA shock load (▲). (A) Survival of (*Pseudomonas stutzeri amp*)cells in reactors 3; (B) concentration of 3-CA in reactors 2 and 3 in the effluent; (C) nitrate concentration in the effluent; (D) ammonium (solid symbols, solid line) and nitrite (open symbols, dotted line) concentrations in the effluent; (E) settlement of the activated sludge, expressed as SVI; (F) COD concentration in the effluent. Values represent the mean and standard error of results from two reactors (n = 2); in some cases, the error bars were too small to illustrate

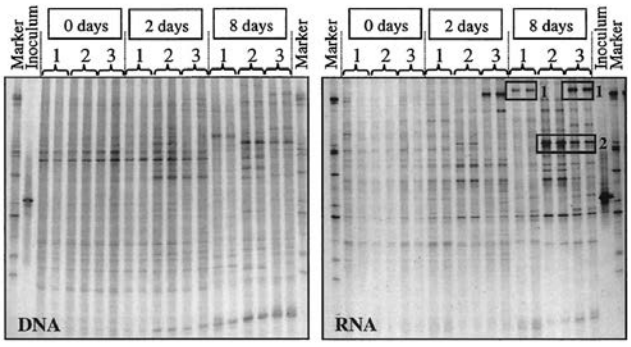

Figure 2. Analysis of the DGGE profiles of the different reactors on days 0，2,and 8 using partial bacterial I6S rRNA gene fragments (bp 338 to 518), based on extracted DNA and RNA. Boxed areas indicate the bands excised and sequenced for further analysis; the accession numbers of the most similar sequences in GenBank are mentioned in the text. Lanes: 1. reactors without inoculate and without 3-CA shock: 2, nonbioaug- mcntcd reactors with 3-CA shock load; 3, bioaugmented reactors with 3-CA shock load

3.2. DGGE Analysis of the *Bacteria*

To relate the observed changes in function to changes in the community structure and diversity, 16S rDNA and 16S rRNA DGGE analyses were performed with bacterial primers. Since days 0, 2, and 8 were considered to be typical for the microbial community, with day 0 representing the community just before disruption, day 2 representing disruption, and day 8 representing recovery, these samples were analyzed by DGGE in detail. Visual comparison of the RNA DGGE patterns at day 8 allowed us to select two bands that were clearly different among the differently treated reactors. On day 8, in nondisturbed reactors 1 and bioaugmented reactors 3, there was a prominent band in the RNA DGGE gel (Figure 2, band 1), with a sequence having low similarity to members of the *Cytophaga- Flavobacter* group (146 of 168 bp with the uncultured bacterial clone AF369713.1, and 98 of 104 bp with *Cytophaga* sp. strain AJ224415.1 [55], a fragment isolated from a nitrifying reactor system). This band was not visible in the patterns of the 3-CA-treated reactors, which could indicate that the corresponding organism was very sensitive to the toxic shock. Another fragment, band 2, present only in reactors receiving 3-CA (reactors 2 and 3), is identical to the sequence of the gram-positive actinomycete *Nostocoida limicola* AF255736.1 (177 of 177 bp; sequence isolated from a bulking filamentous bacterium in a reactor treating industrial waste). The clear presence of this band in the fingerprint might be an

indication that this corresponding organism is more resistant to the 3-CA shock load. The differences between the DGGE patterns based on extracted RNA and DNA were evaluated by cluster analysis and calculation of the Chao2 richness estimator. The RNA-based DGGE patterns for all bacteria contained fewer bands than the DNA-based DGGE patterns (Figure 2). This observation was confirmed by the Chao2 richness estimator, obtained by numerical analysis of the DGGE patterns: the values obtained for the DNA DGGE patterns were always higher than for the RNA DGGE profiles (data not shown). This indicates that not all the microorganisms present were highly active. However, it is also possible that the RNA DGGE analysis was confounded by one or a few strains that produce large amounts of rRNA and thus the RNA concentrations of several other active species may have fallen below the presumed 1% detection limit, typical for PCR-DGGE [47]. On day 0, several faint bands and just one or two dominant ribotypes were present in both DGGE patterns. The DGGE patterns for the DNA and the RNA samples were very reproducible, since only small differences between the patterns from day 0 and from the duplicate reactors were noticeable. Cluster analysis confirmed these observations (Figure 3). During the experiment, certain bands became more dominant while some faint bands became invisible. As a result, fewer bands were detected from day 2 and the Chao 2 richness decreased during the experiment in all reactors compared with day 0 (data not shown). Cluster analysis of the DNA DGGE patterns showed that the reactors on days 0 and 2 formed one large cluster while each reactor on day 8 produced a distinctive group. Cluster analysis of the RNA DGGE revealed three clusters. The samples from day 0 and the control reactors 1 from day 2 formed one cluster. From day 2, the observed changes in the microbial community structure of reactors 2 were different from those of the other reactors. A third cluster consisted of reactors 3 from days 2 and 8 and of reactors 1 from day 8.

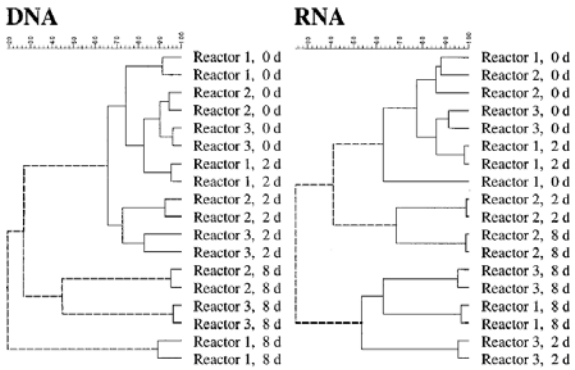

Figure 3. Cluster analysis of the bacterial DGGE patterns based on DNA and RNA samples from the different reactors 1. 2. and 3 (Figure 2). The dendrogram was calculated on *the* basis of the Pearson product-moment correlation coefficient with the UPGMA clustering algorithm. Significant (solid lines) and nonsignificant (dotted lines) clusters were separated by the statistical cluster cutoff method)d. d, days

3.3. DGGE Analysis of AOB

Since the 3-CA shock and the bioprotection had a major influence on the nitrification activity in reactors 2 and 3, a more detailed analysis of the AOB was performed. On day 0 (good nitrification activity before the shock), DGGE patterns obtained with primers for AOB were very similar, even between the RNA and DNA samples (Figure 4). A visual comparison of the RNA DGGE patterns showed that two bands seemed to play a critical role in the nitrification (bands 3 and 4). These two intense bands were excised from the RNA DGGE gel and sequenced (Figure 4). The upper band, band 3, showed highest similarity to an uncultured *Nitrosomonas* strain AJ245752.1 (173 of 173 bp; sequence obtained from a selective enrichment of AOB from a sediment) and to an uncultured member of the β-*Proteobacteria*, AJ299051.1 (177 of 177 bp [56]; sequence of an AOB enriched from a freshwater sediment), while the lower band, band 4, matched with a *Ni-trosococcus/Nitrosomonas* strain (174 of 177 bp were identical to the corresponding sequence of *Nitrosococcus mobilis* AF287297.1 [57], AJ298728.1 [58], and M96403.1 [59] and *Nitrosomonas* sp. strain AF272415.1 [57]). In the lower part of the DGGE gels, a few other bands were present as well, but no effect of the treatments on the corresponding populations were observed. Although nitrification was inhibited in reactors 2 as well as reactors 3, 2 days after the shock load, the RNA DGGE patterns of the AOB community structure differed between these two reactors. On day 2 in reactor 2, band 3 was hardly visible in the RNA DGGE patterns, and after 8 days, both bands 3 and 4 had almost disappeared. In the bioaugmented reactors 3, however, both bands 3 and 4 were still clearly detectable on day 2. Interestingly, a third potential AOB, represented by band 5, identified as an uncultured member of the β-*Proteobacteria*, became more dominant. The DNA sequence of this fragment was identical (171 of 172 bp) to a sequence submitted to GenBank (AJ245760.1, obtained by selective enrichment of ammonia-oxidizing bacteria in freshwater sediments). This DNA fragment was obtained by this group by using the same specific primers for AOB that were used in our study. The first known sequence of an AOB similar to band 5 is *N. mobilis* (155 of 176 bp identical, or 88% similarity; accession number AF287297.1 [57]). By day 8, when nitrification was restored in the bioaugmented reactors 3, the RNA DGGE profiles were similar to their original pattern and the additional band 5 had disappeared.

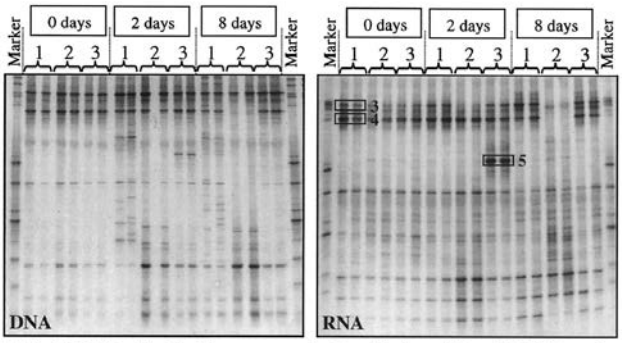

Figure 4. Analysis of the DGGE profiles of the different reactors on days 0, 2, and 8, using partial bacterial 16S rRNA gene fragments, based on DNA and RNA. The gene fragments were obtained by using an AOB-specific PCR with primers CTOl89AB. CT0189C. and CT0653r (Table 1), followed by a second PCR with bacterial primers P338F and P5l8r (Table 1). Bands 3 . 4. and 5 were excised and sequenc'd for further analysis. Lanes: 1, reactors without inoculate and without 3.CA shock; 2. nonbioaugmented reactors with 3. CA shock load; 3. bioaugmented reactors with 3-CA shock load. The accession numbers of the most similar sequencecs in GenBank are mentioned in the text

3.4. Quantification of the AOB by FISH and Real-time PCR

The DGGE analysis showed that shifts occurred in the AOB community. Since it is not possible to obtain quantitative data from the DGGE patterns, real-time PCR and FISH were used to examine the prevalence of the AOB in the activated sludge. On days 0, 2, and 8, the number of rRNA molecules present in the reactors was estimated by amplifying the 16S rRNA cDNA of the *Bacteria* and the AOB from the different reactors and measuring the increasing amounts of amplification products. The relative number of AOB was estimated by dividing the number of AOB rRNA copies by the total number of bacterial rRNA copies (Figure 5). The data showed that the relative number of rRNA copies of the AOB decreased after 2 days, both in the bioaugmented and in the non bioaugmented reactors. At 8 days after the shock load, the number of rRNA copies of the AOB decreased further in the non bioaugmented reactors, while in the bioprotected reactors the number had increased again. To confirm the trend observed in the real-time PCR data, FISH analysis was also applied. From the different reactors on days 0 and 8, the area of all the bacteria and of the AOB was measured and the ratio of AOB and bacteria was calculated. On day 0, clusters of AOB could be observed in the activated sludge flocs and an area-based calculation estimated that 2.23% ± 0.76% of the area consisted of AOB. By day 8, AOB clusters were detected only in the reactors where nitrification was observed, i.e., reactors 1 (1.73% ± 0.76%) and 3 (1.60% ± 0.05%), whereas in reactor 2, almost no AOB flocs were observed (0.47% ± 0.59%). The results of the real-time PCR and the FISH quantification indicate that the number of 16S rRNA molecules of the AOB decreased drastically in reactor 2 from day 0 to day 8, while the populations seemed largely protected by bioaugmentation with the 3-CA degrading strain. This confirms the interpretation formulated above based on the RNA DGGE patterns, i.e., that the nitrifying community had recovered from the 3-CA pulse in the bioaugmented reactors only.

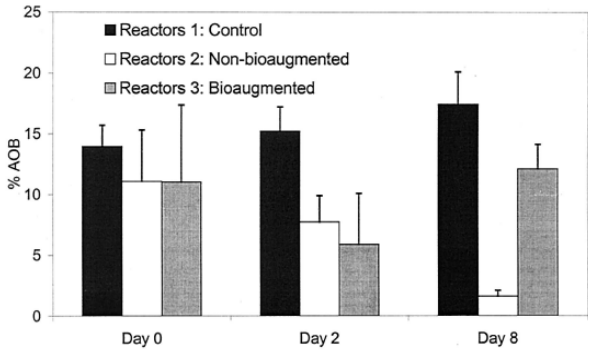

Figure 5. Relative abundance of cDNA of AOB in activated-sludge reactors, as determined by real-time PCR. Values represent the mean and standard error (n = 3)

3.5 Microscopic Analysis of Cell and Floc Morphologies

To explain the altered settlement characteristics of reactors 2 and 3, the floc structures in the different reactors were examined by light microscopy (data not shown). On day 0, a limited number of filaments were present. In the control reactors 1, the sludge floc structure did not change after 8 days and the number of filaments did not increase. However, in the shock-loaded reactors 2 and 3, where an increased SVI was observed, the number of filaments was larger on day 8 than on day 0.

4. Discussion

We investigated the effects of 3-CA shock load on the basic functions of a wastewater treatment reactor and focused on the recovery of major functional activities. Moreover, bioaugmentation by the inoculation of a 3-CA-degrading strain was used to investigate whether rapid 3-CA removal could decrease the recovery period. The most drastic effect of the 3-CA shock load observed was on the nitrification activity. Initially, nitrification was totally inhibited in reactors 2 and 3 where a 3-CA shock load was applied. The non substituted form of 3-CA, aniline, is known to inhibit nitrification [60,61], and, like most inhibitors, aniline inhibits nitrification activity by acting as a suicide substrate for ammonium monooxygenase [62]. As a consequence, reestablishment of the nitrification activity in the activated sludge after the removal of the inhibitor through degradation or washout requires de novo synthesis of the enzymes. After 2 days in the bioaugmented reactors 3, 3-CA was degraded completely, allowing the slow recovery of nitrification activity, which was visible from day 4 (Figure 1). The observed temporal accumulation of nitrite is normal during the startup period of nitrification [63,64]. In the RNA DGGE profiles of the AOB community, an additional very intense band appeared on day 2 in the bioaugmented reactors 3. In the corresponding DNA DGGE patterns of day 2, the species corresponding to this extra band was represented by a weak band but did not appear to be the most numerically dominant. These data, taken together, suggest that this bacterial population represented by band 5 became a relatively more abundant and highly active member of the community. This population may have had a selective advantage over the other two populations, represented by bands 3 and 4. Work by Suwa et al. [65] showed that various *Nitrosomonas* strains isolated from activated sludge could be either sensitive or insensitive to ammonium. The short-term inhibition of nitrification by 3-CA led to an accumulation of ammonium, which may have inhibited the organisms represented by bands 3 and 4. Band 5, which may represent an AOB that is insensitive to higher ammonium concentrations, would then be able to become more dominant and more active. Thus, as the rRNA content of the two initial dominating AOB (bands 3 and 4) decreased relative to band 5, the new band became visible as a large fraction of the total RNA (band 5). From day 4, the ammonium concentration decreased again, such that the nitrification activity by the original AOB (bands 3 and 4) was restored while the other population (band 5) appeared to be outcompeted again. In the non bioaugmented reactor 2, band 5 was never visible since the corresponding organism was probably also inhibited by the high 3-CA concentration. In these reactors 2, the 3-CA was present for 4 days, in contrast to less than 2 days in the bioaugmented reactors 3 (Figure 1B), and thus the entire nitrifying community was apparently inhibited during this time. Although 3-CA levels were undetectable

by day 6, no nitrification recovery was observed in reactors 2. A contact time of 4 days with 3-CA seemed to be critical for the AOB. This was corroborated by the disappearance of the two dominant bacteria of the AOB community on day 8, as indicated in the RNA DGGE patterns for reactors 2. The results of real-time PCR and FISH analysis confirmed the negative effect of the 3-CA exposure on the community of AOB, since hardly any AOB cells or clusters could be detected in reactors 2 on day 8. Nitrification would possibly recover in the non bioaugmented reactors if the experiment were prolonged, allowing the AOB to proliferate again. The higher SVI in reactors 2 and 3 was clearly a result of the 3-CA shock load. Microscopy revealed a larger number of filaments in both reactors, and sequencing of a dominant band in the RNA DGGE profiles of reactors 2 and 3 revealed the presence of an actinomycete (AF255736.1), i.e., *Nostocoida limicola*. This species has been related to the decline of sludge settling properties in a large number of studies [66,67], and an increased number of filaments has been shown to correspond to higher SVI values [66,68,69]. It is well known that actinomycetes exhibit the capacity to metabolize recalcitrant molecules (42). The actinomycete-like filaments in the shock-loaded reactors 2 and 3 may be the result of improved resistance to 3-CA. After the 3-CA shock, a higher COD concentration in the effluent of the non bioaugmented reactors 2 was observed. The heterogeneous nature of wastewaters allows the development of diverse heterotrophic bacterial populations. From day 4, the COD removal was essentially restored; the higher COD concentrations in these reactors on day 4 were presumably due to the residual 3-CA concentration (ca. 150 of the extra 200 mg/liter), which was gradually washed out. The effect of inoculation of *Pseudomonas stuzeri amp* into the shock-loaded reactors was striking: COD removal capacity was not lowered, resulting in a full protection of the activated sludge and COD levels comparable to the non-shocked control reactors 1. There are different factors that can explain the increased COD concentrations in the effluent of the non bioaugmented reactors 2: (i) the indigenous bacteria, responsible for the COD removal, could be temporarily inhibited by the long 3-CA shock; (ii) the protozoa, important predators of bacteria, could be inhibited, resulting in an increased number of dispersed bacteria in the effluent; or (iii) the toxicity of the 3-CA could have resulted in the lysis of a part of the biomass. Some combination of all these factors is also a possible explanation for the increased COD on day 2 in reactors 2. Methods based on direct PCR amplification and analysis of rRNA genes by DGGE or temperature gradient gel electrophoresis (TGGE) are frequently used to examine the microbial community structure and microbial diversity of environmental samples [71,72,73,74]. However, PCR-based techniques can be biased [51]. The number and intensity of bands in a DGGE pattern do not necessarily give an accurate picture of the microbial community. Because of the shortcomings inherent to DGGE based on PCR-amplified rRNA gene sequences, the estimators calculated from the DGGE banding patterns must be interpreted as only an indication and not an absolute measure of the degree of diversity in a bacterial community [72]. Also, one organism may produce more than one DGGE band because of multiple, heterogeneous rRNA operons [75,76,77] and one DGGE band may represent several species with identical partial 16S rDNA sequences [78]. In a mixture of target rRNA genes present at very different concentrations, the less abundant sequences are not amplified sufficiently to be visualized as bands on a DGGE gel, and therefore, the banding pattern reflects only the most abundant rRNA types in the microbial community [47]. This is why the inoculated strain could hardly be seen in the DGGE patterns on day 2 in the bioaugmented reactors 3. On day 8, the inoculated strain was not detectable any more, most probably because its proportion of the total bacterial cell numbers had become too small. In our previous work, the same inoculum was also not visible in the DGGE patterns of bioaugmented activated sludge [41]. Another bias is the shortcoming of primers and probes concerning their specificity. The work of Purkhold et al. [57] clearly demonstrated that at the moment, there is no perfect primer or probe set to study AOB. The CTO primer set used in this study also matches with some non-AOB strains [57], and therefore it cannot be excluded that some of the bands in the DGGE patterns may be not related to AOB. In this study, we used DGGE analysis based on extracted DNA as well as RNA to evaluate changes in the sludge microbial communities. It appears from the bacterial DGGE patterns that the number of numerically dominant populations present was larger than the number of abundant and highly active populations: on day 0, the bacterial richness based on the RNA DGGE patterns was markedly lower than for the DNA DGGE patterns. This suggests a lower bacterial richness among the active numerically dominant populations than among the total (dead, dormant, and active) dominant populations. Some very active populations, visible in the RNA DGGE patterns, can hardly be detected in the DNA DGGE fingerprints. This shows that DNA-based analyses do not al-ways reflect the most active members of the microbial community. DNA obtained from environmental samples could originate from dormant or dead cells [79] or even from free DNA. This is also reflected in the analysis of the AOB: based on the DNA DGGE, only some small differences in the minor bands were visible on days 0 and 2, while the RNA DGGE clearly showed differences in the dominant bands, as discussed above. This difference may reflect differences in the activity of the nitrifying species between these two time points. A similar phenomenon was observed for RNA TGGE fingerprints of grassland soil bacterial communities, which were less diverse than the DNA TGGE fingerprints [80]. Numerical analysis of our DGGE results also indicated that the significant clusters of the RNA DGGE patterns reflect better the metabolic state of the different reactors than the DNA DGGE patterns do. The DNA DGGE cluster analysis showed one large cluster of days 0 and 2, while after 8 days every set of duplicate reactor formed a separate cluster. In contrast, the RNA DGGE analysis resulted in three distinct clusters: (i) all reactors before day 0 and control reactors 1 on day 2, (ii) the shock-loaded and disturbed reactors 2 on days 2 and 8 and (iii) the control reactors 1 on day 8 and the bioaugmented-recovered reactors 3 on days 2 and 8. Therefore, RNA DGGE analysis is appropriate to examine rapidly changing microbial communities while DNA DGGE analysis appears sufficient for slowly evolving, stable communities.

This study has demonstrated that a 3-CA shock load disrupted the basic metabolic functions of activated sludge. Inoculation with a bacterial strain capable of 3-CA mineralization protected the performance of the reactors and allowed a rapid recovery of nitrification. Some of these functional changes were explained by changes in the structure of the overall bacterial community, specifically of the AOB community. Although evaluation of the eventual success of this bioaugmentation strategy at field scale requires further experiments, in particular under conditions of post-shock inoculations, our work clearly indicates that inoculation of wastewater treatment systems subject to toxic shock loads, with a specific degrader of the toxic compound, can result in faster recovery of essential metabolic functions.

References

[1] Seviour R, Nielsen PH (2010) Microbial ecology of activated sludge. London: IWA Publishing Company. 688 p. 2. Bitton G (2011) Wastewater microbiology. Hoboken, NJ: John Wiley and Sons. 746 p.

[2] Graham DW, Smith VH (2004) Designed ecosystem services: Application of ecological principles in wastewater treatment engineering. Front Ecol Environ 4: 199-206.

[3] Wang X, Wen X, Yan H, Ding K, Zhao F, et al. (2011) Bacterial community dynamics in a functionally stable pilot-scale wastewater treatment plant. Bioresour Technol 102: 2352-2357.

[4] Curtis TP, Head IM, Graham DW (2003) Theoretical ecology in engineering biology. Environ Sci Technol 37: 64A-70A.

[5] Wells GF, Park HD, Eggleston B, Francis CA, Criddle CS (2011) Fine-scale bacterial community dynamics and the taxa-time relationship within a full-scale activated sludge bioreactor. Water Res 45: 5476-5488.

[6] Wagner M, Loy A, Nogueira R, Purkhold U, Lee N, et al. (2002) Microbial community composition and function in wastewater treatment plants. Antonie van Leeuwenhoek 81: 665 680.

[7] Kaewpipat K, Grady CPL (2002) Microbial population dynamics in laboratory scale activated sludge reactors. Water Sci Technol 46: 19-27.

[8] Padayachee P, Ismail A, Bux F (2006) Elucidation of the microbial community structure within a laboratory-scale activated sludge process using molecular techniques. Water SA 32: 679-686.

[9] Jenkins D (2008) From total suspended solids to molecular biology tools a personal view of biological wastewater treatment process population dynamics. Water Environ Res 80: 677-687.

[10] Saikaly PE, Stroot PG, Oerther DB (2005) Use of 16S rRNA gene terminal restriction fragment analysis to assess the impact of solids retention time on the bacterial diversity of activated sludge. Appl Environ Microbiol 71: 5814-5822.

[11] Ofit¸eru ID, Lunn M, Curtis TP, Wells GF, Criddle CS, et al. (2010) Combined niche and neutral effects in a microbial wastewater treatment community. Proc Natl Acad Sci U S A 107: 15345-15350.

[12] Sanapareddy N, Hamp TJ, Gonzalez LC, Hilger HA, Fodor AA, et al. (2009) Molecular diversity of a North Carolina wastewater treatment plant as revealed by pyrosequencing. Appl Environ Microbiol 75: 1688-1696.

[13] Fierer N, Lennon JT (2011) The generation and maintenance of diversity in microbial communities. Am J Bot 98: 439-448.

[14] Nemergut DR, Costello EK, Hamady M, Lozupone C, Jiang L, et al. (2011) Global patterns in the biogeography of bacterial taxa. Environ Microbiol 13: 135-144.

[15] Benedict RG, Carlson DA (1971) Aerobic heterotrophic bacteria in activated sludge. Water Res 5: 1023-1030.

[16] Dias FF, Bhat JV (1964) Microbial ecology of activated sludge. Appl Microbiol 12: 412-417.

[17] Lighthart B, Oglesby RT (1969) Bacteriology of an activated sludge wastewater treatment plant: A guide to methodology. J Water Pollut Control Fed 41: R267-R281.

[18] van Veen W (1973) Bacteriology of activated sludge, in particular the filamentous bacteria. Antonie van Leeuwenhoek 39: 189-205.

[19] Eschenhagen M, Schuppler M, Ro¨ske I (2003) Molecular characterization of the microbial community structure in two activated sludge systems for the advanced treatment of domestic effluents. Water Res 37: 3224-3232.

[20] Snaidr J, Amann R, Huber I, Ludwing W, Schleifer K (1997) Phylogenetic analysis and in-situ identification of bacteria in activated sludge. Appl Environ Microbiol 63: 2884-2896.

[21] Wagner M, Amann R, Lemmer H, Schleifer K (1993) Probing activated sludge with oligonucleotides specific for proteobacteria: Inadequacy of culture dependent methods for describing microbial community structure. Appl Environ Microbiol 59: 1520-1525.

[22] Watanabe K, Yamamoto S, Hino S, Harayama S (1998) Population dynamics of phenol-degrading bacteria in activated sludge determined by gyrB-targeted quantitative PCR. Appl Environ Microbiol 64: 1203-1209.

[23] Green JL, Bohannan BJM (2006) Spatial scaling of microbial biodiversity. Trends Ecol Evol 21: 501-507.

[24] Martiny JBH, Bohannan BJM, Brown JH, Colwell RK, Fuhrman JA, et al. (2006) Microbial biogeography: putting microorganisms on the map. Nat Rev Microbiol 4: 102-112.

[25] van der Gast CJ, Jefferson B, Reid E, Robinson T, Bailey MJ, et al. (2006) Bacterial diversity is determined by volume in membrane bioreactors. Environ Microbiol 8: 1048-1055.

[26] Wang X, Wen X, Criddle C, Wells G, Zhang J, et al. (2010) Community analysis of ammonia-oxidizing bacteria in activated sludge of eight wastewater treatment systems. J Environ Sci (China) 22: 627-634.

[27] Loy A, Daims H, Wagner M (2002) Activated sludge: molecular techniques for determining community composition. In: Bitton G, editor. The Encyclopedia of environmental microbiology. Hoboken, NJ: John Wiley and Sons. 26-43.

[28] Onuki M, Satoh H, Mino T, Matsuo T (2000) Application of molecular methods to microbial community analysis of activated sludge. Water Sci Technol 42: 17-22.

[29] Wilderer PA, Bungartz HJ, Lemmer H, Wagner M, Keller J, et al. (2002) Modern scientific methods and their potential in wastewater science and technology. Water Res 36: 370-393.

[30] de los Reyes FL III (2010) Challenges in determining causation in structure function studies using molecular biological techniques. Water Res 44: 4948-4957.

[31] Jones PA, Schuler AJ (2010) Seasonal variability of biomass density and activated sludge settle ability in full-scale wastewater treatment systems. Chem Eng J 164: 16-22.

[32] Carvalho G, Lemos PC, Oehmen A, Reis MAM (2007) Denitrifying phosphorus removal: Linking the process performance with the microbial community structure. Water Res 41: 4383-4396.

[33] Briones A, Raskin L (2003) Diversity and dynamics of microbial communities in engineered environments and their implications for process stability. Curr Opin Biotechnol 14: 270-276.

[34] Gentile ME, Jessup CM, Nyman JL, Criddle CS (2007) Correlation of functional instability and community dynamics in denitrifying dispersed-growth reactors. Appl Environ Microbiol 73: 680-690.

[35] Curtis TP, Sloan WT (2006) Towards the design of diversity: stochastic models for community assembly in wastewater treatment plants. Water Sci Technol 54: 227-236.

[36] Daims H, Taylor MW, Wagner M (2006) Wastewater treatment: a model system for microbial ecology. Trends Biotechol 24: 483-489.

[37] Prosser JI, Bohannan BJ, Curtis TP, Ellis RJ, Firestone MK, et al. (2007) The role of ecological theory in microbial ecology. Nat Rev Microbiol 5: 384-392.

[38] Acinas SG, Rodríguez-Valera F, Pedrós-Alió C (1997) Spatial and temporal variation in marine bacterioplancton diversity as shown by RFLP fingerprinting of PCR amplified 16S rDNA. FEMS Microbiol Ecol 24: 27-40

[39] Martínez-Murcia AJ, Acinas SG, Rodríguez-Valera F (1995) Evaluation of prokaryotic diversity by restrictase digestion of 16S rDNA directly amplified from hipersaline environments. FEMS Microbiol Ecol 17: 247-256

[40] Moyer CL, Dobbs FC, Karl DM (1994) Estimation of diversity and community structure through restriction fragment length polymorphism distribution analysis of bacterial 16S rRNA genes from a microbial mat at an active, hydrothermal vent system, Loihi Seamount, Hawaii. Appl Environ Microbiol 60: 871-879

[41] Boon, N., J. Goris, P. De Vos, W. Verstraete, and E. M. Top. 2000. Bioaugmentation of activated sludge by an indigenous 3-

chloroaniline degrading *Comamonas testosteroni* strain, I2 *gfp*. Appl. Environ. Microbiol. 66: 2906-2913.

[42] Greenberg, A. E., L. S. Clesceri, and A. D. Eaton (ed.). 1992. Standard methods for the examination of water and wastewater, 18th ed. American Public Health Association, American Water Works Association, and Water Environment Federation, Washington D.C.

[43] Boon, N., J. Goris, P. De Vos, W. Verstraete, and E. M. Top. 2001. Genetic diversity among 3-chloroaniline and aniline degrading strains of the *Comamonadaceae*. Appl. Environ. Microbiol. 67: 1107-1115.

[44] Amann, R. I. 1995. In situ identification of micro-organisms by whole cell hybridization with rRNA-targeted nucleic acid probes, p. 1-15. *In* A. D. L. Akkermans, J. D. van Elsas, and F. J. de Bruijn (ed.), Molecular microbial ecology manual. Kluwer Academic Publishers, Dordrecht, The Netherlands.

[45] Griffiths, R. I., A. S. Whiteley, A. G. O'Donnell, and M. J. Bailey. 2000. Rapid method for coextraction of DNA and RNA from natural environments for analysis of ribosomal DNA-and rRNA-based microbial community composition. Appl. Environ. Microbiol. 66: 5488-5491.

[46] Kowalchuk, G. A., P. L. E. Bodelier, G. H. J. Heilig, J. R. Stephen, and H. J. Laanbroek. 1998. Community analysis of ammonia-oxidising bacteria, in relation to oxygen availability in soils and root-oxygenated sediments, using PCR, DGGE and oligonucleotide probe hybridisation. FEMS Microbiol. Ecol. 27: 339-350.

[47] Boon, N., W. De Windt, W. Verstraete, and E. M. Top. 2002. Evaluation of nested PCR-DGGE (denaturing gradient gel electrophoresis) with group specific 16S rRNA primers for the analysis of bacterial communities from different wastewater treatment plants. FEMS Microbiol. Ecol. 39: 101-112.

[48] Muyzer, G., E. C. de Waal, and A. Uitterlinden. 1993. Profiling of complex microbial populations using denaturing gradient gel electrophoresis analysis of polymerase chain reaction-amplified genes coding for 16S rRNA. Appl. Environ. Microbiol. 59: 695-700.

[49] Colwell, R. K. 1997. EstimateS: statistical estimation of species richness and shared species from samples, version 5. User's Guide and application published at http://viceroy.eeb.uconn.edu/estimates.

[50] Colwell, R. K., and J. A. Coddington. 1994. Estimating terrestrial biodiversity through extrapolation. Philos. Trans. R. Soc. London Ser. B 345: 101-118.

[51] Hughes, B. J., J. J. Hellmann, T. H. Ricketts, and B. J. M. Bohannan. 2001. Counting the uncountable: statistical approaches to estimating microbial diversity. Appl. Environ. Microbiol. 67: 4399-4406.

[52] Suzuki, M., and S. Giovannoni. 1996. Bias caused by template annealing in the amplification of mixtures of 16S rRNA genes by PCR. Appl. Environ. Microbiol. 62: 625-630.

[53] Heid, C., J. Stevens, K. Livak, and P. Williams. 1996. Real time quantitative PCR. Genome Res. 6: 986-994.

[54] Biesterfeld, S., L. Figueroa, M. Hernandez, and P. Russell. 2001. Quantification of nitrifying bacterial populations in a full-scale trickling filter using fluorescent *in situ* hybridisation. Water Environ. Res. 73: 329-338.

[55] Daims, H., N. B. Ramsing, K. H. Schleifer, and M. Wagner. 2001. Cultivation-independent, semiautomatic determination of absolute bacterial cell numbers in environmental samples by fluorescence in situ hybridization. Appl. Environ. Microbiol. 67: 5810-5818.

[56] Logemann, S., J. Schantl, S. Bijvank, M. van Loosdrecht, J. G. Kuenen, and M. S. M. Jetten. 1998. Molecular microbial diversity in a nitrifying reactor system without sludge retention. FEMS Microbiol. Ecol. 27: 239-249.

[57] Bollmann, A., and H. J. Laanbroek. 2001. Continuous culture of ammoniaoxidising bacteria at low ammonium concentrations. FEMS Microbiol. Ecol. 37: 211-221.

[58] Purkhold, U., A. Pommerening-Roser, S. Juretschko, M. C. Schmid, H. P. Koops, and M. Wagner. 2000. Phylogeny of all recognized species of ammonia oxidizers based on comparative 16S rRNA and amoA sequence analysis: Implications for molecular diversity surveys. Appl. Environ. Microbiol. 66: 5368-5382.

[59] Aakra, A., J. B. Utaker, A. Pommerening-Roser, H. P. Koops, and I. F. Nes. 2001. Detailed phylogeny of ammonia-oxidizing bacteria determined by rDNA sequences and DNA homology values. Int. J. Syst. Evol. Microbiol. 51: 2021-2030.

[60] Head, I. M., W. D. Hiorns, T. M. Embley, A. J. McCarthy, and J. R. Saunders. 1993. The phylogeny of autotrophic ammonia-oxidising bacteria as determined by analysis of 16S ribosomal RNA gene sequences. J. Gen. Microbiol. 139: 1147-1153.

[61] Ficara, E., and A. Rozzi. 2001. pH-stat titration to assess nitrification inhibition. J. Environ. Eng. 127: 698-704.

[62] McCarthy, G. W. 1999. Modes of action of nitrification inhibitors. Biol. Fertil. Soils 29: 1-9.

[63] Gheewala, S. H., and A. P. Annachhatre. 1997. Biodegradation of aniline. Water Sci. Technol. 36: 53-63.

[64] Lekang, O.-I., and H. Kleppe. 2000. Efficiency of nitrification in trickling filters using different filter media. Aquacult. Eng. 21: 181-199.

[65] Villaverde, S., F. Fdz-Olanco, and P. A. Garcia. 2000. Nitrifying biofilm acclimation to free ammonia in submerged biofilters. Water Res. 34: 602-610.

[66] Suwa, Y., Y. Imamura, T. Suzuki, T. Tashiro, and Y. Urushigawa. 1994. Ammonia-oxidizing bacteria with different sensitivities to (NH4)2SO4 in activated sludges. Water Res. 28: 1523-1532.

[67] Lemmer, H., G. Lind, E. Muller, M. Schade, and B. Ziegelmayer. 2000. Scum in activated sludge plants: Impact of non-filamentous and filamentous bacteria. Acta Hydrochim. Hydrobiol. 28: 34-40.

[68] Wanner, J., I. Ruzickova, P. Jetmarova, O. Krhutkova, and J. Paraniakova. 1998. A national survey of activated sludge separation problems in the Czech Republic: Filaments, floc characteristics and activated sludge metabolic properties. Water Sci. Technol. 37: 271-279.

[69] Madoni, P., D. Davoli, and G. Gibin. 2000. Survey of filamentous microorganisms from bulking and foaming activated-sludge plants in Italy. Water Res. 34: 1767-1772.

[70] Nielsen, J. L., L. H. Mikkelsen, and P. H. Nielsen. 2001. *In situ* detection of cell surface hydrophobicity of probe-defined bacteria in activated sludge. Water Sci. Technol. 43: 97-103.

[71] McCarthy, A. J., and S. T. Williams. 1992. Actinomycetes as agents of biodegradation in the environment—a review. Gene 115: 189-192.

[72] Curtis, T. P., and N. G. Craine. 1998. The comparison of the diversity of activated sludge plants. Water Sci. Technol. 37: 71-78.

[73] Eichner, C. A., R. W. Erb, K. N. Timmis, and I. Wagner-Do¨bler. 1999. Thermal gradient gel electrophoresis analysis of bioprotection from pollutant shocks in the activated sludge microbial community. Appl. Environ. Microbiol. 65: 102-109.

[74] Muyzer, G., and K. Smalla. 1998. Application of denaturing gradient gel electrophoresis (DGGE) and temperature gradient gel electrophoresis (TGGE) in microbial ecology. Antonie Leeuwenhoek 73: 127-141.

[75] van Elsas, J. D., G. F. Duarte, A. S. Rosado, and K. Smalla. 1998. Microbiological and molecular biological methods for monitoring microbial inoculants and their effects in the soil environment. J. Microbiol. Methods 32: 133-154.

[76] Cilia, V., B. Lafay, and R. Christen. 1996. Sequence heterogeneities among 16S ribosomal RNA sequences, and their effect on phylogenetic analyses at the species level. Mol. Biol. Evol. 13: 451-461.

[77] Nubel, U., B. Engelen, A. Felske, J. Snaidr, A. Wieshuber, R. I. Amann, W. Ludwig, and H. Backhaus. 1996. Sequence heterogeneities of genes encoding 16S rRNAs in *Paenibacillus polymyxa* detected by temperature gradient gel electrophoresis. J. Bacteriol. 178: 5636-5643.

[78] Rainey, F. A., N. L. WardRainey, P. H. Janssen, H. Hippe, and E. Stackebrandt. 1996. *Clostridium paradoxum* DSM 7308(T) contains multiple 16S rRNA genes with heterogeneous intervening sequences. Microbiology 142: 2087-2095.

[79] Vallaeys, T., E. Topp, G. Muyzer, V. Macheret, G. Laguerre, A. Rigaud, and G. Soulas. 1997. Evaluation of denaturing gradient gel electrophoresis in the detection of 16S rDNA sequence variation in rhizobia and methanotrophs. FEMS Microbiol. Ecol. 24: 279-285.

[80] Josephson, K. L., C. P. Gerba, and T. L. Pepper. 1993. Polymerase chain reaction of nonviable bacterial pathogens. Appl. Environ. Microbiol. 59: 3513-3515.

[81] Øvreas, L., L. Forney**,** F. L. Daae, and V. Torsvik**.** 1997. Distribution of bacterioplankton in meromictic lake Saelevannet, as determined by denaturing gradient gel electrophoresis of PCR-amplified gene fragments coding for 16S rRNA. Appl. Environ. Microbiol. 63: 3367-3373.

[82] Mobarry, B., M. Wagner, V. Urbain, B. Rittmann, and D. Stahl. 1996. Phylogenetic probes for analyzing abundance and spatial

organization of nitrifying bacteria. Appl. Environ. Microbiol. 62: 2156-2162.

[83] Amann, R. I., B. J. Binder, R. J. Olson, S. W. Chisholm, R. Devereux, and D. A. Stahl. 1990. Combination of 16S rRNA-targeted oligonucleotide probes with flow cytometry for analyzing mixed microbial populations. Appl. Environ. Microbiol. 56: 1919-1925.

[84] Daims, H., A. Bruhl, R. Amann, K. H. Schleifer, and M. Wagner. 1999. The domain-specific probe EUB338 is insufficient for the detection of all *Bacteria*: development and evaluation of a more comprehensive probe set. Syst. Appl. Microbiol. 22: 434-444.